Biochemistry and Biophysics Reports 13 (2018) 7–11

Contents lists available at ScienceDirect

Biochemistry and Biophysics Reports

journal homepage: www.elsevier.com/locate/bbrep

# Biophotonic markers of malignancy: Discriminating cancers using wavelength-specific biophotons

Nirosha J. Murugan[a,b,c,*], Nicolas Rouleau[b,c], Lukasz M. Karbowski[c], Michael A. Persinger[b,c]

[a] Tufts University, 200 Boston Ave, Medford, MA 02155, USA
[b] Quantum Biomolecular Laboratory, Laurentian University, Sudbury, Ontario, Canada P3E 2C6
[c] Behavioural Neuroscience Programs, Laurentian University, Sudbury, Ontario, Canada P3E 2C6

## ABSTRACT

Early detection is a critically important factor when successfully diagnosing and treating cancer. Whereas contemporary molecular techniques are capable of identifying biomarkers associated with cancer, surgical interventions are required to biopsy tissue. The common imaging alternative, positron-emission tomography (PET), involves the use of nuclear material which poses some risks. Novel, non-invasive techniques to assess the degree to which tissues express malignant properties are now needed. Recent developments in biophoton research have made it possible to discriminate cancerous cells from normal cells both in vitro and in vivo. The current study expands upon a growing body of literature where we classified and characterized malignant and non-malignant cell types according to their biophotonic activity. Using wavelength-exclusion filters, we demonstrate that ratios between infrared and ultraviolet photon emissions differentiate cancer and non-cancer cell types. Further, we identified photon sources associated with three filters (420-nm, 620-nm., and 950-nm) which classified cancer and non-cancer cell types. The temporal increases in biophoton emission within these wavelength bandwidths is shown to be coupled with intrisitic biomolecular events using Cosic's resonant recognition model. Together, the findings suggest that the use of wavelength-exclusion filters in biophotonic measurement can be employed to detect cancer in vitro.

## 1. Introduction

Malignant growths, left undetected, can become increasingly difficult to treat or remove. It is therefore imperative that technologies are developed which can detect malignancies before cells invade neighboring tissues or metastases are generated elsewhere in the body. Though molecular techniques are currently available which detect biomolecules within specimens obtained by biopsy, recent advances have produced alternative non-invasive detection methods which do not require surgery. Among them, biophotonic techniques represent a novel approach which makes use of light that is derived from cells to differentiate malignant and non-malignant tissues [11,2]. Shimizu et al. [20] have not only measured weak biophoton emissions from transplanted tumors but observed differences in these emission profiles amongst different types of tumors. Dotta et al. [5] have recently demonstrated that, using a serious of wavelength exclusion filters in vitro, the temporal emission of these photons can be correlated to precise biomolecular cascades that are associated with cancer processes. Even elevations in biophoton emissions from serum or urine obtained from cancer patients have shown to display distinctive profiles compared to the bio-fluids obtained from healthy individuals [1,2].

Cellular derived ultra-weak biophoton emissions can be used as a biological marker which could represent an important step toward the establishment of novel detection methods in oncology. Imaging tissues without the use of nuclear materials, as is required in positron-emission tomography (PET), could reduce the time necessary to detect and diagnosis cancers, however, it also displays several shortcomings such as exclusion of vulnerable populations (i.e. patients who are pregnant or breastfeeding) or the cost effectiveness/maintenance of the imaging tool [10,14]. Even utilizing biophotons as a method for pathological detection possess its own obstacles. The central challenge here is that biophoton markers must be characterized and separated from normal cellular biophotonic activity as well as extraneous sources of noise. The Cosic Resonant Recognition Model (RRM) represents a practical solution in this regard [3,4]. This physiciomathemtical model was used to determine the characteristics frequencies of a protein using the energy of the delocalized electrons from its linear amino acid sequence. Irena Cosic developed this model to investigate the significant resemblance between functionally similar proteins using the idea of electromagnetic resonance. She later identified that based on these coherent domains,

* Corresponding author at: Tufts University, 200 Boston Ave, Medford, MA 02155, USA.
*E-mail address:* nirosha.murugan@tufts.edu (N.J. Murugan).

https://doi.org/10.1016/j.bbrep.2017.11.001
Received 13 July 2017; Received in revised form 26 August 2017; Accepted 10 November 2017

frequencies can emerge that are founded on the basis of electromagnetics or light. These proteins that drive molecular pathways are highly associated with the peak frequencies within the ultraviolet through the visible to the near infrared range as has been shown by Dotta et al. [5]. In the same study, they showed that the dominant frequency of select proteins can be manipulated by activators and inhibitors, proving that these frequencies are strongly correlated to the specific proteins.

There are many classes of proteins whose over or under expression can be predictive of malignancy. Therefore resonant signatures of biophotonic activity which are known to pair reliably with key biomolecular events involved in cancer can be used as biophotonic markers. Whereas temporal patterns of photon emissions can be indicative of malignancy or human presence [23,24,7], wavelength should be considered as a critical parameter. The wavelength of a photon is proportional to its energy. Biophoton emissions are known to reliably increase in cells which display increased metabolic activity or energy consumption [19,6,7,9]. Increased metabolism drives chemical reactions which release detectable photonic energy. It is proven that tumors consume a lot of energy – as such they'll be brighter and the bright light will have key frequencies embedded. In this present study, we harness these increases in biophoton intensity and energy to discriminate between healthy and malignant cells.

## 2. Materials and methods

### 2.1. Cell cultures

Both normal and malignant cell lines used in this study have been derived and obtained from the American Type Culture Collection (ATCC). The source type of each cell line can be seen in Table 1.

All cell cultures were maintained in 150 × 20 mm cell culture plates using Dulbecco's Modified Essential Medium supplemented with 10% fetal bovine serum, 100 μg/m streptomycin, and 100 U/ml penicillin. The cell cultures were incubated at 37 °C in 5% $CO_2$. For experimentation, the cell monolayers were washed with room temperate, neutral pH PBS, cultivated by incubation in a .25% trypsin solution, collected by centrifugation and seeded onto 60 × 15 mm culture plates. A final cell density in each culture plate prior to biophoton emission recording was $1.0 \times 10^6$ cells each containing a total medium volume of 2.5 $cm^3$.

### 2.2. Detection of wavelength specific photon emission

Immediately after removal from the incubator, a single plate was placed onto the aperture of a Model DM 0090-C digital photon multiplier tube (PMT) (SENS-TECH Sensory Technologies), located in an adjacent room. The wavelength bandwidth or this PMT was between 280–975 nm. Depending on the wavelength of emission to be measured, the appropriate band-pass filter (Chroma Technologies), was placed on top of the aperture before exposure above the culture dish (Fig. 1). The band-pass filters used in this study were 370 nm, 420 nm, 500 nm, 620 nm, 790 nm, and 950 nm – each rated with a filter error range of ± 5 nm. These filters were selected based upon the Cosic RRM equivalencies of proteins tied to physiological processes as shown by Dotta et al. [5]. The entire experimental detection system was placed into a darkened wooden box, covered with black material to ensure no environmental light pollution would alter the sensitivity of the PMT. The typical dark counts or background ambient recordings obtained for this PMT were in the range of 15–25 photon units per second. Measurements were recorded by the DM0101 Counter timer Module with a sampling rate of 2.5 s for 22.5 h. Each cell line was measured in triplicate with the presence of each of the 6 filters and without the presence of any filter to measure the total photon emission from the cell.

**Table 1**
Complete list of cell lines used in this study and their source.

| *Acronym* | *Derivation* |
|---|---|
| *B16 BL6* | Murine melanoma |
| *MDA MB 231* | mammary adenocarcinoma derived from metastatic site |
| MCF 7 | mammary adenocarcinoma |
| AsPC-1 | pancreatic metastatic |
| *HEK 293* | embryonic kidney |
| HBL 100 | mammary |

## 3. Results

Classifying cell types as malignant (cancer) or non-malignant (non-cancer), a two-way analysis of variance (ANOVA) identified a filter by cell type interaction, $F(6,102) = 2.69$, $p < .005$, $\eta^2 = .21$. The source of variance was identified as significantly decreased photon emissions from non-cancerous cells ($M = 6752.38$, $SEM = 66.18$) relative to cancerous cells ($M = 7958.22$, $SEM = 262.87$) when selecting for the 420-nm wavelength filter applied to the PMT, $t(12) = -2.82$, $p < .05$, $r^2 = .40$ (Fig. 2). Equality of variances as inferred by Levene's Test were assumed ($p > .05$) and the reliability of the phenomenon was robust in triplicate.

Employing discriminant analyses to classify photon emissions into nominal categories of "cancerous" and "non-cancerous" cell type aggregates was unsuccessful without the application of appropriate filters to the PMT, $\Lambda = .99$, $\chi^2(1) = 1.84$, $p > .05$. However, selecting for photon data which had been filtered before interfacing with the PMT and therefore subject to the exclusion of all light with the exception of a single wavelength could differentiate the two systems. Of the 6 filters, 3 were associated with photon counts which could be used to discriminate cancerous and non-cancerous cell type aggregates: 420-nm ($\Lambda = .66$, 78.6% correct classification), 950-nm ($\Lambda = .72$, 70.6% correct classification), and 620-nm ($\Lambda = .76$, 70.6% correct classification). Selecting for cases associated with a combination of the three significant filter applications (420-nm, 620-nm, and 950-nm) produced results which were comparable to individual applications, $\Lambda = .87$, $\chi^2(1) = 6.16$, $p < .05$, classifying 69% of cases. However, when systematically removing cell types from the binary model, the removal of HBL cells increased the classification result to 92%, $\Lambda = .43$, $\chi^2(1) = 29.67$, $p > .001$. Whereas the classification of photon emissions from non-cancerous cells was moderate (63%), 100% ($n = 30$) of cases associated with cancer cell emissions were correctly classified.

A significant, positive linear relationship was identified between standardized photon emissions and the wavelength of the applied PMT filter for non-cancer cells, $r = .48$, $p < .005$, $rho = .41$, $p < .05$ (Fig. 3). The trend suggested that, for non-cancer cells, greater proportions of emitted photons were within the near-infrared red range which decreased moderately with successively shorter wavelengths. In contrast, a negative linear relationship was identified between the same variables for cancer cells, $r = -.27$, $p < .05$, $rho = -.33$, $p < .05$ (Fig. 2). From this perspective, cancer cells displayed a reverse trend – emitting greater proportions of near-UV range photons with decreasing counts as wavelength increased. It was therefore apparent that a ratio of photon counts obtained using the UV (370 nm) and IR (950 nm) filters could serve as a measure of malignancy. An examination of the 23 h period of measurement revealed a discrete time period between the 13th and 15th hours of measurement during which standardized UV-IR ratios for non-cancer cells were elevated relative to cancer cells, $t(18) = 3.72$, $p < .005$, $r^2 = .44$. UV-IR photon emission ratios displayed by non-cancer and cancer cells during 1 h periods before and after this discrete window were not significantly different ($p > .05$).

Examining hourly photon counts, an ANOVA identified a 5 h period during which individual cell types differed significantly ($p < .05$) with a peak effect size of 43% during the 13th hour of measurement, $F(4,28) = 4.61$, $p < .01$ (Fig. 4). Homogeneous subsets revealed that HBL-100 and HEK-293T cells were reliably different from MDA-MB-231 cells

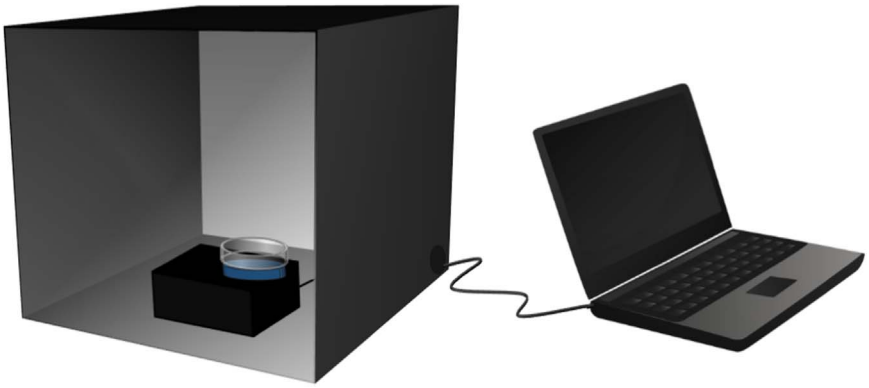

**Fig. 1.** Schematic for wavelength-specific biophoton emission detection within a darkened wooden box. The wavelength specific band-pass filter (blue disc) that only allows the emission of light of either 370 nm, 420 nm, 500 nm, 620 nm, 790 nm, or 950 nm to be detected by the PMT (black box) is placed below a confluent plate of malignant or healthy cells (clear dish).

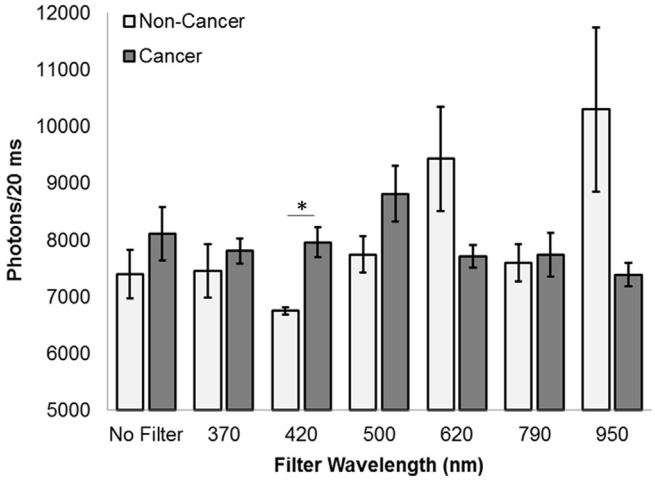


**Fig. 2.** Photon counts per 20 ms. increment for non-cancer (light) and cancer (dark) cells as a function of the applied PMT filter. A significant difference after accommodating for homogeneity of variance is indicated ($p < .05$).

over the 5 h period where the non-cancer cells displayed more extreme standardized photon count scores relative to MDA-MB-231 ($p < .05$). This was likely due to the highly-variable and wavelength-independent standardized photon counts displayed by MDA-MB-231 cells which, in Fig. 3, are compared to those displayed by HEK-293T cells.

## 4. Discussion

Our results demonstrated that malignant (cancer) and non-malignant (non-cancer) cells could be discriminated as a function of raw photon counts if the PMT device was pre-filtered to exclude all wavelengths of light with the exception of 420-nm, 620-nm, and 950-nm. Whereas moderate classifications were achieved for both independent filters and a combination of filters, our most accurate classification was only achieved when removing HBL100 cells. Further, we identified a clear correlate of cancer and non-cancer cells which were inverse proportions of IR and UV photon sources. Though the correlations were weak, the trend reversal indicated that a ratio of IR to UV sources could be useful in further classifications of malignancy based upon biophoton emissions. Finally, we identified a temporal discriminant factor, standardized photon counts approximately 13 h into recording, between the non-cancerous cell group (i.e., HBL100 and HEK-293T) and MDA-MB-231 cells. This period of measurement was marked by a separation of the standardized photon count trends where non-cancer cell types displayed decreased values relative to MDA-MB-231 cells.

The exclusion-filters which produced optimal classification (420 nm, 620 nm, 950 nm) could be significant for several reasons. As described by Dotta et al. [5] these wavelengths are coupled to distinct families of biomolecules that drive signal cascades. Namely, 420 nm, using the Cosic RRM, has been correlated to proteins stemming from SOS response proteins, and actin/myosin molecules. The 620 nm is associated with lysosomes whilst 950 nm is associated with signal proteins. Each of these family of proteins have all been experimentally validated to be directly involved with the formation [21,8], proliferation [18] and spread [12,13] of various malignant systems.

It was observed that the removal of HBL100 cells from the discriminant analysis produced the most accurate classification function. This could suggest that photon emissions from HBL100 cells are, in fact, not representative of the group in which they were originally classified

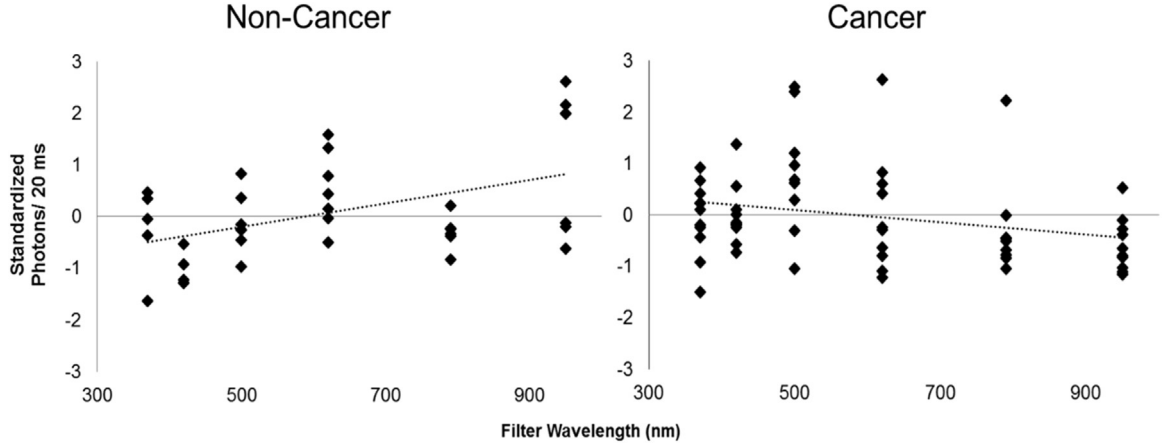


**Fig. 3.** Non-cancer (left) and cancer (right) cells display opposite linear relationships between standardized photon emissions per 20 ms increment and the wavelength of the applied PMT filter.

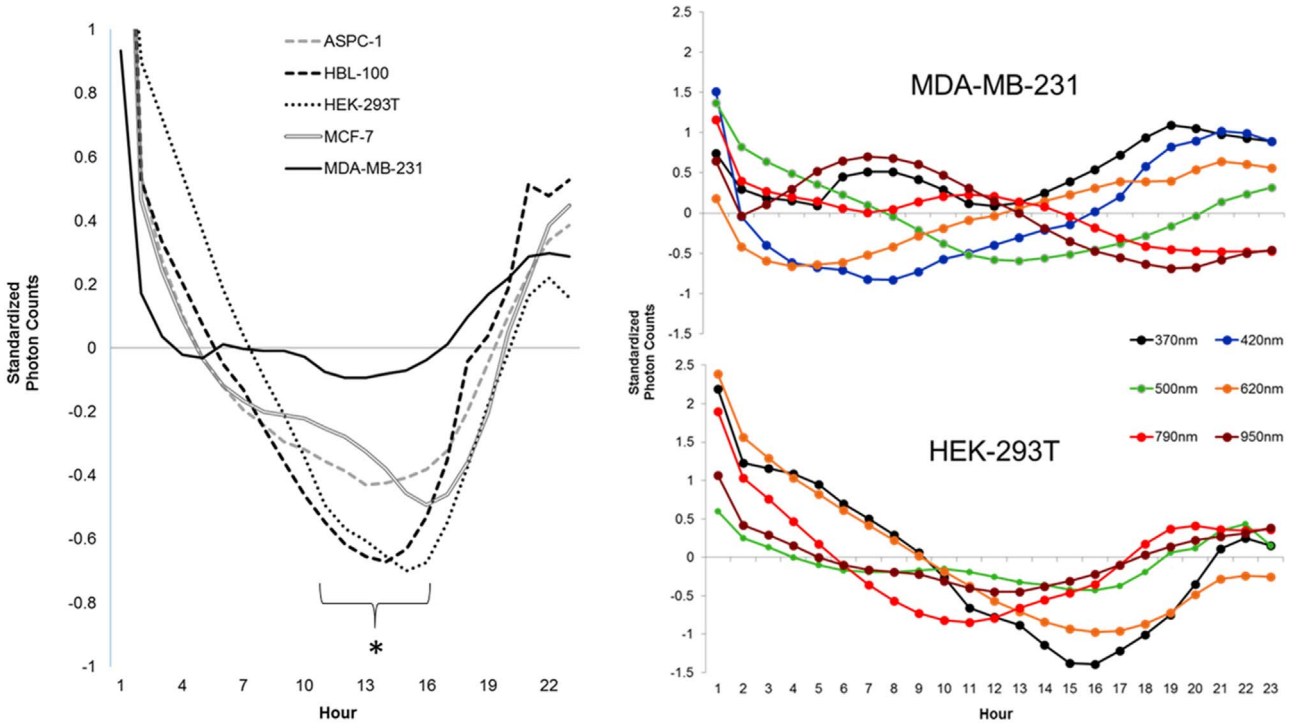


**Fig. 4.** A series of significant differences during a consecutive 5 h period (*p < .05) during which HEK-293T and HBL-100 cells displayed reduced averaged standardized photon counts per 20 ms increment relative to MDA-MB-231 cells (left). Profiles of MDA-MB-231 and HEK-293T cells revealed that the former cell type displayed greater variability over time and between PMT filter conditions relative to the latter cell type (right).

(i.e. non-cancer). There is evidence to suggest that HBL100 cells are significantly different than HEK293 cells in many respects [17], one of which is that they are not healthy breast-derived cells, but are transformed non-tumorigenic cells, incorrectly classified unknown origins [16].

The opposed relationships between the wavelengths of the applied exclusion filters and standardized photon counts per unit time indicate that biophotons emitted from cancer and non-cancer sources are fundamentally different in their spectral distributions. Whereas non-cancer cells displayed predominantly IR-centered biophoton emissions with proportional decreases as a function of deviating wavelengths, the reverse was true of cancer cells, displaying predominantly UV-centered biophoton emissions. Similar observations have been reported in the literature, indicating that considerable shifts of wavelength are typical of the transition between malignant and non-malignant cell groups [22,5]. It should be noted that the distribution of points for cancer cells (Fig. 3) are relatively variable as compared to non-cancer cells. This level of heterogeneity could be indicative of the increased number of cells within the non-cancer cell group aggregate or could be indicative of intrinsic variability characteristic of malignant cells. Distributions of wavelength-specific photon emissions from cancer cells over time as visualized in Fig. 4 support the latter possibility.

In general, the results demonstrate that biophoton emissions from cancer and non-cancer cells differ fundamentally as a function of wavelength and temporal patterning. These observations are entirely predicted by Cosic's RRM which would presuppose the pairing of emissions and specific biomolecular events which are known to differ as a function of malignancy. That there are biophysical correlates tied to cell types which are known to harbor disparate biomolecular signatures is unsurprising given recent discoveries [15,5]. However, as demonstrated here the utility of band-pass or exclusion filters as tools to enhance the classification accuracy of PMT data could provide a basis for new imaging technologies to detect or screen for signatures indicative of malignancy in vitro and in vivo. Further, the use of IR-UV ratios as crude determinants of malignancy could be a novel and potent method of supplementing said detection. Further studies should aim to expand the spatial resolution of the exclusion filters to accommodate intermediate wavelengths. By identifying key wavelengths which reliably differentiate cancer and non-cancer cells, biophoton classifications of malignancy can become increasingly powerful as a screening tool.

## Appendix A. Transparency document

Supplementary data associated with this article can be found in the online version at http://dx.doi.org/10.1016/j.bbrep.2017.11.001.

## References

[1] T. Amano, M. Kobayashi, B. Devaraj, M. Usa, H. Inaba, Ultraweak biophoton emission imaging of transplanted bladder cancer, Urol. Res. 23 (5) (1995) 315–318.
[2] C.P. Chilton, G.A. Rose, Urinary chemiluminescence – an evaluation of its use in clinical practice, Br. J. Urol. 56 (1984) 650–654.
[3] I. Cosic, D. Cosic, K. Lazer, Analysis of tumor necrosis factor function using the resonant recognition model, Cell. Biochem. Biophys. 75 (2) (2016) 175–180.
[4] I. Cosic, Macromolecular bioactivity: is it resonant interaction between macromolecules? Theory and applications, IEEE Trans. Biomed. Eng. 41 (1994) 1101–1114.
[5] B.T. Dotta, N.J. Murugan, L.M. Karbowski, R.M. Lafrenie, M.A. Persinger, Shifting wavelengths of ultraweak photon emissions from dying melanoma cells: their chemical enhancement and blocking are predicted by Cosic's theory of resonant recognition model for macromolecules, Naturwissenschaften 101 (2) (2014) 87–94.
[6] B.T. Dotta, C.A. Buckner, D. Cameron, R.F. Lafrenie, M.A. Persinger, Biophoton emission from cell cultures: biochemical evidence for the plasma membrane as the primary source, Gen. Physiol. Biophys. 30 (3) (2011) 301–309.
[7] B.T. Dotta, L.M. Karbowski, N.J. Murugan, D.A.E. Vares, M.A. Persinger, Ultra-weak photon emissions differentiate malignant cells from nonmalignant cells in vitro, Arch. Cancer Res. 4 (2) (2016) 1–4.
[8] A.L. Edinger, C.B. Thompson, Defective autophagy leads to cancer, Cancer Cell 4 (6) (2003) 422–424.
[9] D. Fels, Cellular communication through light, PLOS One. 4 (4) (2009) 1–8 (e5086).
[10] A. Gallamini, C. Zwarthoed, A. Borra, Positron emission tomography (pet) oncology, Cancers (Basel) 6 (4) (2014) 1821–1889.
[11] G.C. Gisler, J. Diaz, N. Duran, Observation on blood plasma chemiluminescence in normal subjects and cancer patietnts, Arq. Biol. Technol. 26 (3) (1983) 345–352.
[12] K. Glunde, Z.M. Bhujwalla, S.M. Ronen, Choline metabolism in malignant transformation, Nat. Rev. Cancer 11 (12) (2011) 835–848.
[13] K. Glude, M.A. Jacobs, A.P. Pathak, D. Artemov, Z.M. Bhujwalla, Molecular and

functional imaging of breast cancer, NMR Biomed. 22 (2008) 92–103.
[14] M.M. Hanasono, L.D. Kunda, G.M. Segall, G.H. Ku, D.J. Terris, Uses and limitations of FDG positron emission tomography in patients with head and neck cancer, Laryngoscope 109 (6) (1999) 880–885.
[15] L.M. Karbowski, N.J. Murugan, M.A. Persinger, Experimental evidence that specific photon energies are "stored" in malignant cells for an hour: the synergism of weak magnetic field-led wavelength pulses, Biol. Med. 8 (1) (2016) 1–8.
[16] M. Lacroix, Persistent use of "false" cell lines, Int. J. Cancer 122 (2008) 1–4.
[17] Y.C. Lin, M. Boone, L. Meuris, I. Lemmens, N.V. Roy, A. Soete, J. Reumers, M. Moisse, S. Plaisance, R. Dramanac, J. Chen, F. Speleman, D. Lambrechts, Y.V. de Peer, J. Travernier, N. Callewaert, Genome dynamics of the human embryonic kidney 293 lineage in response to cell biology manipulations, Nat. Commun. 5 (2014) 1–12 (4767).
[18] K.H. Maclean, F.C. Dorsey, J.L. Cleveland, M.B. Kastan, Targeting lysosomal degradation induces p53-dependent cell death and prevents cancer in mouse models of lymphomagenesis, J. Clin. Investig. 118 (1) (2008) 79–88.
[19] F.A. Popp, Coherent photon storage of biological systems, in: F.A. Popp, G. Becker, H.L. Konig, W. Peschka (Eds.), Electromagnetic Bioinformation, Urban and Schwarzenbeg, Munich, 1979, pp. 123–149.
[20] S. Shimizu, N. Miyamoto, T. Matsuura, Y. Fujii, M. Umezawa, K. Umegaki, K. Hiramoto, H. Shirato, A proton beam therapy system dedicated to spot-scanning increases accuracy with moving tumors by real-time imaging and gating and reduces equipment size, PLoS One 9 (4) (2014) e94971.
[21] M.D. Sutton, B.T. Smith, V.G. Godoy, G.C. Walker, The SOS response: recent insights into umuDC-dependent mutagenesis and DNA damage tolerance, Annu. Rev. Genet. 34 (1) (2000) 479–497.
[22] J. Tafur, E.P.A. Van Wijk, R. Van Wijk, P.J. Mills, Biophoton detection and low-intensity light therapy. a potential clinical partnership, Photomed. Laser Surg. 28 (1) (2010) 23–30.
[23] M. Takeda, M. Kobayashi, M. Takayama, S. Suzuki, T. Ishida, K. Ohnuki, T. Moriya, N. Ohuchi, Biphoton detection as a novel technique for cancer imaging, Cancer Sci. 95 (8) (2004) 656–661.
[24] D.A.E. Vares, B.T. Dotta, K.S. Saroka, L.M. Karbowski, N.J. Murugan, M.A. Persinger, Spectral power densities and whole body photon emissions from human subjects sitting in hyper-darkness, Arch. Cancer Res. 4 (2) (2016) 1–4.